



Exploring high-temperature superconductivity in the extended Hubbard model with antiferromagnetic tendencies

Zhipeng Sun ^{*}*Beijing Computational Science Research Center, Beijing 100193, China*Hai-Qing Lin[†]*Beijing Computational Science Research Center, Beijing 100193, China
and Department of Physics, Zhejiang University, Hangzhou 310058, China* (Received 15 April 2023; revised 6 August 2023; accepted 11 December 2023; published 4 January 2024)

The enigma of unconventional superconductivity in doped cuprates presents a formidable challenge in the realm of condensed matter physics. Recent findings of strong near-neighbor attractions in one-dimensional cuprate chains suggest a new avenue for investigating cuprate superconductors. Consequently, we revisited the superconductivity in the extended Hubbard model at the mean-field level. Anticipating a prevalence of antiferromagnetic order due to strong local Coulomb repulsion, our calculations reveal the coexistence of superconducting and antiferromagnetic orders across a wide range of doping at sufficiently low temperatures. The mean-field results capture some key features of cuprate superconductors, including d -wave pairing symmetry, a dome-shaped dependence of T_c on doping, and higher superconducting transition temperatures. Additionally, we observe a nearly proportional relationship between T_c and the strength of the nearest-neighbor attraction, reminiscent of experimental findings at the FeSe/SrTiO₃ interface. The mean-field results suggest that the extended Hubbard model could be the appropriate framework for investigating cuprate superconductivity and offer insights for more precise calculations within this model in the future.

DOI: [10.1103/PhysRevB.109.035107](https://doi.org/10.1103/PhysRevB.109.035107)

I. INTRODUCTION

The unconventional superconductivity in doped cuprate materials has been a focal point in condensed matter physics [1–4] since its discovery in 1986 [5]. In contrast to conventional metal-based superconductors well-described by BCS theory [6], the unconventional nature of these materials manifests in various aspects such as narrow-band electronic structures, superconducting (SC) transition temperatures T_c exceeding the McMillan limit [7], and dominantly d -wave pairing symmetry [4]. The dome-shaped variation of T_c with doping concentration, along with unusual isotope effects [8,9], introduces additional complexities requiring explanation. Furthermore, above T_c , cuprate superconductors exhibit strongly correlated phenomena such as the pseudogap [10], the stripe order [11], and strange metallic behavior [12] that defy the traditional Ginzburg-Landau framework, adding a layer of mystery to the mechanism.

Faced with these puzzles, the prevailing view among researchers is that superconductivity in cuprates does not arise from the electron-phonon mechanism advocated by BCS theory. Instead, there has been a shift towards exploring new pairing mechanisms. Based on the electronic structure of cuprates, their physics is believed to be describable by the Hubbard model or its extended versions [2,13]. A key and highly controversial question is whether superconductivity

can exist in the simplest two-dimensional Hubbard model. On this matter, there are both negative and affirmative studies, but a consensus remains elusive to date [14–17]. In a recent review [18], Singh summarized several leading theories supporting the existence of superconductivity in the Hubbard model. While these theories have achieved notable successes, there are also aspects that remain unsatisfactorily addressed.

A crucial argument against the electron-phonon mechanism in cuprate superconductors is the McMillan limit [19]. However, it is important to clarify that the McMillan formula relies on two fundamental premises: first, the electronic density of states near the Fermi level is nearly constant, and second, the electron-phonon coupling constant is much smaller than the Debye frequency and the bandwidth. Regarding strong electron-phonon coupling, it is meaningful for superconductors under high pressure [20], but its relevance for exploring room pressure superconductivity may be limited. Regarding the density of states, in the presence of Van Hove singularities (VHSs), the dependence of T_c on the electron-phonon coupling constant is much different from the BCS formula. The influence of VHSs has been extensively discussed in numerous papers [21–24].

The impact of a divergent density of states on T_c was elucidated more clearly in a short article [25]. The authors explored a simple two-band BCS Hamiltonian, with one of the bands exhibiting a flat dispersion, within the mean-field approximation. They observed that T_c is nearly proportional to the pairing coupling constant, in stark contrast to the conventional BCS exponential law. Building on this insight, some researchers have initiated investigations into the potential

^{*}zpsun@csrc.ac.cn[†]haiqing0@csrc.ac.cn

for room temperature superconductivity on flat-band systems [26,27].

Supporting evidence for the electron-phonon mechanism appeared in recent experiments on one-dimensional cuprate chains [28]. The experimental group reported the synthesis and spectroscopic analysis of the one-dimensional cuprate $\text{Ba}_{2-x}\text{Sr}_x\text{CuO}_{3+d}$ over a wide range of hole doping. The results of angle-resolved photoemission experiments fail to match predictions of the simple Hubbard model, while an additional strong near-neighbor attraction quantitatively explains experiments for all accessible doping levels. This attraction may arise from the coupling to phonons, and several related works followed [29,30]. Nevertheless, as suggested by the group, the minimal model for cuprate superconductivity is likely the two-dimensional extended Hubbard model, which contains the nearest-neighbor attraction. Despite extensive research on superconductivity within this model before the experimental discovery [31–34], attention has been rekindled [35,36].

Given the lack of efficient and conclusive solvers for the general cases of the two-dimensional extended Hubbard model, we resorted to mean-field methods to revisit this model, acknowledging that the results may be subject to debate. Taking into account the strong local Coulomb repulsion, we assumed that the system has an antiferromagnetic (AFM) tendency. As a result, across a wide range of doping at sufficiently low temperatures, SC and AFM orders coexist. We found that the mean-field calculations can capture some features of cuprate superconductors, such as the d -wave preference, the dome-shaped dependence of T_c on doping, and higher T_c . Particularly striking was the discovery of an almost proportional relationship between T_c and the strength of the nearest-neighbor attraction, which was evidenced at the FeSe/SrTiO₃ interface [37]. We conjecture that this proportional relationship arises from the VHSs near the Fermi energy. Our mean-field results suggest that the extended Hubbard model could be the appropriate framework for investigating cuprate superconductivity and are expected to offer insights for more precise calculations within this model in the future.

This paper is structured as follows. In Sec. II, we outline the mean-field treatment of the extended Hubbard model and derive the gap equation near T_c . Next, in Sec. III, we compute T_c over a broad range of parameters and examine its characteristics. Then in Sec. IV, we compare our results with previous theoretical studies and experimental findings and engage in a discussion of the implications. Finally, a summary is given in Sec. V.

II. MODEL AND METHOD

We investigate the extended Hubbard model with strong local repulsion U and nearest-neighbor attraction $|V|$ on a two-dimensional square $\mathcal{V} = L \times L$ lattice, whose Hamiltonian reads

$$\hat{H} = -t \sum_{\alpha,r,\delta} \hat{c}_{\alpha,r+\delta}^\dagger \hat{c}_{\alpha,r} - \mu \sum_r \hat{\rho}_r + U \sum_r \hat{n}_{\uparrow,r} \hat{n}_{\downarrow,r} - \frac{|V|}{2} \sum_{r,\delta} \hat{\rho}_{r+\delta} \hat{\rho}_r. \quad (1)$$

Here $\hat{c}_{\alpha,r}^\dagger$ ($\hat{c}_{\alpha,r}$) is the fermionic creation (annihilation) operator with spin α at lattice site r , $\hat{n}_{\alpha,r} \equiv \hat{c}_{\alpha,r}^\dagger \hat{c}_{\alpha,r}$ is the spin-selective density operator, and $\hat{\rho}_r = \hat{n}_{\uparrow,r} + \hat{n}_{\downarrow,r}$ is the charge density operator. δ represents the vectors linking nearest neighbors, t is the nearest-neighbor hopping strength, and μ is the chemical potential.

A. General mean-field framework

Within the symmetry-broken Hartree-Fock framework, the local interacting term can be reduced to

$$U \sum_r (n_{\uparrow,r} \hat{n}_{\downarrow,r} + \hat{n}_{\uparrow,r} n_{\downarrow,r}) + U \sum_r (\hat{c}_{\uparrow,r}^\dagger \hat{c}_{\downarrow,r}^\dagger \Delta_r + \text{H.c.}). \quad (2)$$

Here the local mean fields are defined as $n_{\alpha,r} \equiv \langle \hat{n}_{\alpha,r} \rangle$ and $\Delta_r = \langle \hat{c}_{\downarrow,r} \hat{c}_{\uparrow,r} \rangle$. In terms of the mean-field charge density $\rho_r = n_{\uparrow,r} + n_{\downarrow,r}$ and the mean-field z -spin density $m_r = \frac{1}{2}(n_{\uparrow,r} - n_{\downarrow,r})$, $n_{\alpha,r}$ can be expressed as $\frac{1}{2}\rho_r + \epsilon^\alpha m_r$, with $\epsilon^\uparrow = 1$ and $\epsilon^\downarrow = -1$. H.c. indicates the Hermitian conjugate. The mean-field approximation for the nonlocal interacting term is given by

$$-|V| \sum_{r,\delta} \rho_{r+\delta} \hat{\rho}_r + |V| \sum_{\alpha,r,\delta} \hat{c}_{\alpha,r+\delta}^\dagger \hat{c}_{\alpha,r} n'_{\alpha,\delta,r} - \frac{|V|}{2} \sum_{\alpha,\alpha',r,\delta} (\hat{c}_{\alpha,r+\delta}^\dagger \hat{c}_{\alpha',r}^\dagger \Delta'_{\alpha',\alpha,\delta,r} + \text{H.c.}). \quad (3)$$

Here the nonlocal mean fields are defined as $n'_{\alpha,\delta,r} \equiv \langle \hat{c}_{\alpha,r}^\dagger \hat{c}_{\alpha,r+\delta} \rangle$ and $\Delta'_{\alpha',\alpha,\delta,r} \equiv \langle \hat{c}_{\alpha',r} \hat{c}_{\alpha,r+\delta} \rangle$.

Replacing the U term by Eq. (2) and V term by Eq. (3), we obtain the mean-field Hamiltonian $\hat{H}_{\text{MF}} = \hat{H}_0 + \hat{H}_{\text{SC}}$. Here the “normal” part takes the form

$$\hat{H}_0 = - \sum_{\alpha,r,\delta} \tilde{t}_{r,r+\delta} \hat{c}_{\alpha,r+\delta}^\dagger \hat{c}_{\alpha,r} - \sum_{\alpha,r} \tilde{\mu}_r \hat{c}_{\alpha,r}^\dagger \hat{c}_{\alpha,r}, \quad (4)$$

with the effective hopping $\tilde{t}_{r,r+\delta} = t - |V| n'_{\alpha,\delta,r}$ and effective chemical potential $\tilde{\mu}_r = \mu + \sum_\delta |V| \rho_{r+\delta} - (\frac{1}{2} \rho_r - \epsilon^\alpha m_r) U$. The SC term reads

$$\hat{H}_{\text{SC}} = \left(U \sum_r \hat{c}_{\uparrow,r}^\dagger \hat{c}_{\downarrow,r}^\dagger \Delta_r - |V| \sum_{r,\delta} \hat{c}_{\uparrow,r+\delta}^\dagger \hat{c}_{\downarrow,r}^\dagger \Delta'_{\delta,r} - \frac{|V|}{2} \sum_{\alpha,r,\delta} \hat{c}_{\alpha,r+\delta}^\dagger \hat{c}_{\alpha,r}^\dagger \Delta'_{\alpha,\delta,r} \right) + \text{H.c.} \quad (5)$$

Here $\Delta'_{\delta,r} = \langle \hat{c}_{\downarrow,r} \hat{c}_{\uparrow,r+\delta} \rangle$ and $\Delta'_{\alpha,\delta,r} = \langle \hat{c}_{\alpha,r} \hat{c}_{\alpha,r+\delta} \rangle$ are the nonlocal unequal-spin and equal-spin pairing mean fields, respectively.

The mean-field Hamiltonian \hat{H}_{MF} is quadratic with respect to fermionic operators, thus enabling the establishment of the self-consistent equations for the mean fields. By solving the equations, the mean fields can be calculated, and desired physical quantities can be obtained.

B. AFM ansatz in the normal phase

The mean-field equations can yield various symmetry-broken solutions. However, due to the strong local repulsive interaction, we assume that above T_c , the system is either in

the pure AFM phase or in the Fermi liquid phase. Under this assumption, the mean spin density takes the form $m_r = me^{i\mathbf{Q}\cdot\mathbf{r}}$, with $\mathbf{Q} = (\pi, \pi)$ and $m \geq 0$. In addition, we simplify the problem as much as possible by setting $\rho_r = \rho$ and $n'_{\alpha,\delta,r} = \frac{1}{2}\rho'$. The order parameters in the normal (non-SC) phase are then $\rho = \frac{1}{\mathcal{V}} \sum_{\alpha,k} \langle \hat{c}_{\alpha,k}^\dagger \hat{c}_{\alpha,k} \rangle$, $\rho' = \frac{1}{2\mathcal{V}} \sum_{\alpha,k} \langle \hat{c}_{\alpha,k}^\dagger \hat{c}_{\alpha,k} \rangle \gamma_k$, and $m = \frac{1}{2\mathcal{V}} \sum_{\alpha,k} \epsilon^\alpha \langle \hat{c}_{\alpha,k}^\dagger \hat{c}_{\alpha,k+\mathbf{Q}} \rangle$. Here $\gamma_k = \cos k_x + \cos k_y$ is s wave symmetric.

The normal part [Eq. (4)] of the mean-field Hamiltonian is then simplified as

$$\hat{H}_0 = \sum_{\alpha,k} (-2\tilde{t}\gamma_k - \tilde{\mu}) \hat{c}_{\alpha,k}^\dagger \hat{c}_{\alpha,k} - \sum_{\alpha,k} \epsilon^\alpha U m \hat{c}_{\alpha,k}^\dagger \hat{c}_{\alpha,k+\mathbf{Q}}, \quad (6)$$

where $\tilde{t} = t - \frac{1}{2}|V|\rho'$ is the renormalized nearest-neighbor hopping strength and $\tilde{\mu} = \mu - \frac{1}{2}U\rho + 4|V|\rho$ is the renormalized chemical potential. In the absence of SC orders where $\hat{H}_{\text{MF}} = \hat{H}_0$, we can introduce the Bogoliubov transformation:

$$\begin{bmatrix} \hat{c}_{\uparrow,-\mathbf{p}} \\ \hat{c}_{\uparrow,-\mathbf{p}+\mathbf{Q}} \end{bmatrix} = \begin{bmatrix} \cos \frac{\theta_p}{2} & -\sin \frac{\theta_p}{2} \\ \sin \frac{\theta_p}{2} & \cos \frac{\theta_p}{2} \end{bmatrix} \begin{bmatrix} \hat{a}_{1,\mathbf{p}} \\ \hat{a}_{2,\mathbf{p}} \end{bmatrix}, \quad (7a)$$

$$\begin{bmatrix} \hat{c}_{\downarrow,\mathbf{p}} \\ \hat{c}_{\downarrow,\mathbf{p}+\mathbf{Q}} \end{bmatrix} = \begin{bmatrix} \cos \frac{\theta_p}{2} & \sin \frac{\theta_p}{2} \\ -\sin \frac{\theta_p}{2} & \cos \frac{\theta_p}{2} \end{bmatrix} \begin{bmatrix} \hat{a}_{3,\mathbf{p}} \\ \hat{a}_{4,\mathbf{p}} \end{bmatrix}. \quad (7b)$$

Here \mathbf{p} is confined to half of the first Brillouin zone, and $\theta_p \in [0, \frac{\pi}{2})$ is s wave symmetric, determined by $\cot \theta_p = \frac{2\tilde{t}}{U m} \gamma_p$ if $m \neq 0$ and $\theta_p \equiv 0$ otherwise. By virtue of

Eq. (7), \hat{H}_0 is diagonalized as $\hat{H}_0 = \sum_{i,\mathbf{p}} \tilde{h}_p^i \hat{a}_{i,\mathbf{p}}^\dagger \hat{a}_{i,\mathbf{p}}$, where $\tilde{h}_p^i = [\xi_{p,-}, \xi_{p,+}, -\xi_{p,-}, -\xi_{p,+}]$, with the effective dispersions $\xi_{p,\pm} = \pm \sqrt{4\tilde{t}^2 \gamma_p^2 + U^2 m^2} - \tilde{\mu}$. The normal mean fields above the critical temperature T_c can then be solved from mean-field equations.

C. Ansatz for SC order parameters

Taking into account the existence of AFM order, we make the following ansatz for SC order parameters: the local $\Delta_r = \Delta$, the nonlocal equal-spin $\Delta'_{\alpha,\delta,r} = 0$, and the nonlocal unequal-spin $\Delta'_{\delta,r} = \Delta'_{\delta,0} + \Delta'_{\delta,\mathbf{Q}} e^{i\mathbf{Q}\cdot\mathbf{r}}$. The order parameters involved are given by $\Delta = \frac{1}{\mathcal{V}} \sum_k \langle \hat{c}_{\downarrow,k} \hat{c}_{\uparrow,-k} \rangle$, $\Delta'_{\delta,0} = \frac{1}{\mathcal{V}} \sum_k \langle \hat{c}_{\downarrow,k} \hat{c}_{\uparrow,-k} \rangle e^{ik\cdot\delta}$, and $\Delta'_{\delta,\mathbf{Q}} = \frac{1}{\mathcal{V}} \sum_k \langle \hat{c}_{\downarrow,k+\mathbf{Q}} \hat{c}_{\uparrow,-k} \rangle e^{ik\cdot\delta}$. The SC part [Eq. (5)] of the mean-field Hamiltonian is then simplified as

$$\begin{aligned} \hat{H}_{\text{SC}} = & \left(U \sum_k \hat{c}_{\uparrow,-k}^\dagger \hat{c}_{\downarrow,k}^\dagger \Delta - |V| \sum_{\delta,k} \hat{c}_{\uparrow,-k}^\dagger \hat{c}_{\downarrow,k}^\dagger \Delta'_{\delta,0} e^{-ik\cdot\delta} \right. \\ & \left. - |V| \sum_k \hat{c}_{\uparrow,-k}^\dagger \hat{c}_{\downarrow,k+\mathbf{Q}}^\dagger \Delta'_{\delta,\mathbf{Q}} e^{-ik\cdot\delta} \right) + \text{H.c.} \quad (8) \end{aligned}$$

With Eqs. (6) and (8), the mean-field Hamiltonian takes the quadratic form $\hat{H}_{\text{MF}} = \sum_{i,j,\mathbf{p}} \hat{c}_p^{i\dagger} h_p^{i,j} \hat{c}_p^j$, where $\hat{c}_p^{j\dagger} = [\hat{c}_{\uparrow,-\mathbf{p}}^\dagger, \hat{c}_{\downarrow,-\mathbf{p}}^\dagger, \hat{c}_{\uparrow,\mathbf{p}+\mathbf{Q}}^\dagger, \hat{c}_{\downarrow,\mathbf{p}+\mathbf{Q}}^\dagger]$ and $h_p^{i,j}$ is a 4×4 matrix, given as

$$h_p^{i,j} = \begin{bmatrix} -2\tilde{t}\gamma_p - \tilde{\mu} & -Um & U\Delta - |V|X_{0,\mathbf{p}} & -|V|X_{\mathbf{Q},\mathbf{p}} \\ -Um & 2\tilde{t}\gamma_p - \tilde{\mu} & |V|X_{\mathbf{Q},\mathbf{p}} & U\Delta + |V|X_{0,\mathbf{p}} \\ U\Delta^* - |V|X_{0,\mathbf{p}}^* & |V|X_{\mathbf{Q},\mathbf{p}}^* & 2\tilde{t}\gamma_p + \tilde{\mu} & -Um \\ -|V|X_{\mathbf{Q},\mathbf{p}}^* & U\Delta^* + |V|X_{0,\mathbf{p}}^* & -Um & -2\tilde{t}\gamma_p + \tilde{\mu} \end{bmatrix}. \quad (9)$$

Here the order parameters $X_{0,\mathbf{p}}$ and $X_{\mathbf{Q},\mathbf{p}}$ are defined as

$$X_{0,\mathbf{p}} = \sum_{\delta} \Delta'_{\delta,0} e^{-i\mathbf{p}\cdot\delta}, \quad X_{\mathbf{Q},\mathbf{p}} = \sum_{\delta} \Delta'_{\delta,\mathbf{Q}} e^{-i\mathbf{p}\cdot\delta}. \quad (10)$$

Note that both $X_{0,\mathbf{p}}$ and $X_{\mathbf{Q},\mathbf{p}}$ have only *four* independent components.

With the Bogoliubov transformation (7), the mean-field Hamiltonian can be expressed as $\hat{H}_{\text{MF}} = \sum_{i,j,\mathbf{p}} \hat{a}_{i,\mathbf{p}}^\dagger \tilde{h}_p^{i,j} \hat{a}_{j,\mathbf{p}}$, with $\tilde{h}_p^{i,j}$ given by the following matrix:

$$\tilde{h}_p^{i,j} = \begin{bmatrix} \xi_{p,-} & 0 & A_p & B_p \\ 0 & \xi_{p,+} & -B_p & C_p \\ A_p^* & -B_p^* & -\xi_{p,-} & 0 \\ B_p^* & C_p^* & 0 & -\xi_{p,+} \end{bmatrix}. \quad (11)$$

The undetermined variables A_p , B_p , and C_p are given by

$$A_p = -|V|X_{0,\mathbf{p}} + |V| \sin \theta_p X_{\mathbf{Q},\mathbf{p}} + U \cos \theta_p \Delta, \quad (12a)$$

$$B_p = U \sin \theta_p \Delta - |V| \cos \theta_p X_{\mathbf{Q},\mathbf{p}}, \quad (12b)$$

$$C_p = |V|X_{0,\mathbf{p}} + |V| \sin \theta_p X_{\mathbf{Q},\mathbf{p}} + U \cos \theta_p \Delta. \quad (12c)$$

After diagonalizing the matrix \tilde{h}_p , we can construct the SC gap equations.

D. SC gap equations at the critical point

Near the critical temperature T_c , the parameters A_p , B_p , and C_p are all small, so all quantities can be approximated to first order with respect to them. The SC gap equations can be derived and are as follows:

$$\begin{aligned} \Delta = & -\frac{1}{\mathcal{V}} \sum_p [(A_p F_p^- + C_p F_p^+) \cos \theta_p \\ & + 2B_p F_p' \sin \theta_p], \quad (13a) \end{aligned}$$

$$\Delta'_{\delta,0} = -\frac{1}{\mathcal{V}} \sum_p e^{i\mathbf{p}\cdot\delta} (A_p F_p^- - C_p F_p^+), \quad (13b)$$

$$\begin{aligned} \Delta'_{\delta,\mathbf{Q}} = & \frac{1}{\mathcal{V}} \sum_p e^{i\mathbf{p}\cdot\delta} [(A_p F_p^- + C_p F_p^+) \sin \theta_p \\ & - 2B_p F_p' \cos \theta_p]. \quad (13c) \end{aligned}$$

Here the bubble diagram F are defined as

$$F_p^\pm = \frac{1}{2\xi_{p,\pm}} \tanh \frac{\beta\xi_{p,\pm}}{2},$$

$$F'_p = \frac{1}{\xi_{p,+} + \xi_{p,-}} \frac{1}{2} \left(\tanh \frac{\beta\xi_{p,-}}{2} + \tanh \frac{\beta\xi_{p,+}}{2} \right). \quad (14)$$

By combining Eqs. (10), (12), and (13), we obtain a *ninth*-order homogeneous linear equation set. Based on the condition for the existence of a nonzero solution to the equation set, we can determine T_c and hence explore the physical properties at the SC boundary.

E. Reduction of gap equations by symmetries

As mentioned above, both $X_{0,p}$ and $X_{Q,p}$ defined by Eq. (10) have only *four* independent components; they can be decomposed as

$$X_{0,p} = X_{0,\gamma}\gamma_p + X_{0,\eta}\eta_p + X_{0,v^+}v_p^+ + X_{0,v^-}v_p^-,$$

$$X_{Q,p} = X_{Q,\gamma}\gamma_p + X_{Q,\eta}\eta_p + X_{Q,v^+}v_p^+ + X_{Q,v^-}v_p^-. \quad (15)$$

Here $\gamma_p = \cos p_x + \cos p_y$ exhibits *s*-wave symmetry, $\eta_p = \cos p_x - \cos p_y$ exhibits *d*-wave symmetry, and $v_p^\pm = \sin p_x \pm \sin p_y$ exhibits *p*-wave symmetry. Due to these symmetries, the system of equations for Δ , $X_{0,\varphi}$, and $X_{Q,\varphi}$ ($\varphi = \gamma, \eta, v^+, v^-$) can be decomposed into *four* smaller subsystems.

For a pure *d* wave or *p* wave, the system of equations takes the form

$$\begin{bmatrix} X_{0,\varphi} \\ X_{Q,\varphi} \end{bmatrix} = \begin{bmatrix} M^{11} & M^{12} \\ M^{21} & M^{22} \end{bmatrix} \begin{bmatrix} X_{0,\varphi} \\ X_{Q,\varphi} \end{bmatrix}. \quad (16)$$

Here the elements of the 2×2 matrix M are given by

$$M^{11} = \frac{|V|}{\mathcal{V}} \sum_p \varphi_p^2 (F_p^- + F_p^+),$$

$$M^{12} = M^{21} = -\frac{|V|}{\mathcal{V}} \sum_p \varphi_p^2 (F_p^- - F_p^+) \sin \theta_p,$$

$$M^{22} = \frac{|V|}{\mathcal{V}} \sum_p \varphi_p^2 [\sin^2 \theta_p (F_p^- + F_p^+) + 2 \cos^2 \theta_p F_p']. \quad (17)$$

Based on the condition for the existence of a nonzero solution to Eq. (16), we can obtain T_c for the onset of *d*-wave and *p*-wave pairing instabilities. Additionally, it is worth noting that $X_{Q,\varphi} \neq 0$ implies that the nonlocal SC order is subject to spatial modulation. The gap equation for pure *s*-wave pairing is given in the Appendix.

F. Summary of mean-field formulation

Through a general mean-field treatment of the extended Hubbard model's Hamiltonian (1), we obtain the mean-field Hamiltonian $\hat{H}_{\text{MF}} = \hat{H}_0 + \hat{H}_{\text{SC}}$, where \hat{H}_0 is given by Eq. (4) and \hat{H}_{SC} is given by Eq. (5). Further assumptions lead to the simplification of \hat{H}_{MF} into the form $\hat{H}_{\text{MF}} = \hat{c}_p^{i,\dagger} h_p^{i,j} c_p^j$, where h is a 4×4 matrix as given by Eq. (9). Near the critical temperature T_c , we derive the SC gap equation, provided by Eq. (13). Finally, considering the spatial symmetry of the SC

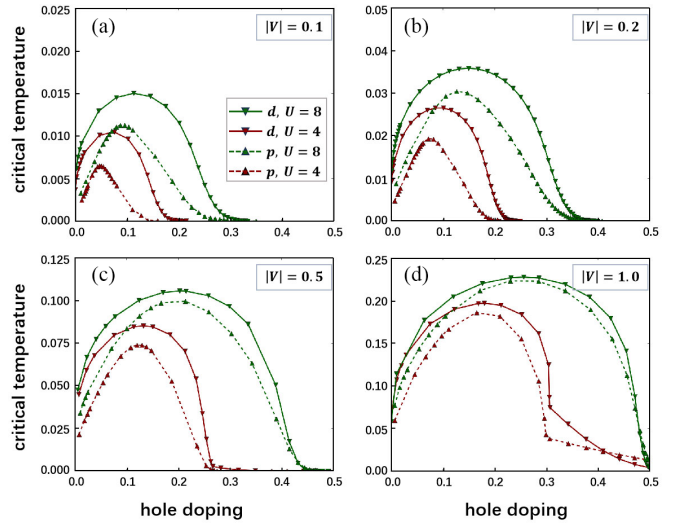


FIG. 1. Critical temperature versus hole doping for *d*-wave instability and *p*-wave instability at varying values of U (4.0, 8.0) and $|V|$ (0.1, 0.2, 0.5, 1.0).

order parameter, the SC gap equation is simplified to Eq. (16) for both *d*-wave and *p*-wave cases.

III. NUMERICAL RESULTS

A. Numerical implementation

The numerical calculations are all performed on a 512×512 square lattice. We set $t = 1$ as the unit of energy and consider only the case $\rho < 1$. The parameter range under consideration is based on the experimental results for cuprate chains [28], where $U \sim 8t$ and $|V| \sim t$. Considering that there is not enough experimental evidence to indicate the presence of strong near-neighbor attractions in two-dimensional cuprates, we will consider a wider range of values for $|V|$.

In the details of implementation, we treat $\mu' = \tilde{\mu} + Um$ as a tunable parameter. For a given μ' , we employ the bisection method to find the temperature T_c at which the largest eigenvalue of the 2×2 matrix M , corresponding to Eq. (16), equals 1. Then other quantities of interest can be obtained.

B. Factors influencing T_c

We focus on factors influencing T_c . First, we plot T_c for *d*-wave and *p*-wave pairing instabilities versus the doping $1 - \rho$ in Fig. 1. Here we choose two sets of U values (4.0, 8.0) and four sets of $|V|$ values (0.1, 0.2, 0.5, 1.0). The plot exhibits *three* key features of T_c : The curve of T_c versus doping forms a dome shape. T_c is positively correlated with local repulsion U , but the relationship is not strong. T_c demonstrates a positive correlation with the nearest-neighbor attraction $|V|$, and the dependence is statistically significant. In addition, *d*-wave instability is generally more prevalent than *p*-wave instability.

To further investigate the dependence of T_c on the nearest-neighbor attraction $|V|$, we plot the optimal T_c versus $|V|$ at varying values of U (4.0, 8.0, 16.0) in Fig. 2, together with the optimal doping. Notably, T_c is almost proportional to $|V|$, and $T_c \sim 0.25|V|$ when U and $|V|$ are both sufficiently large. This

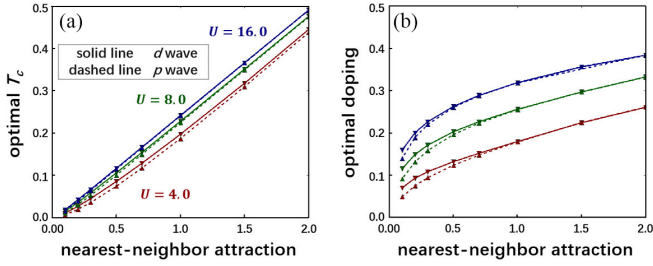


FIG. 2. Optimal critical temperature and hole doping versus nearest-neighbor attraction for d -wave instability and p -wave instability at varying values of U (4.0, 8.0, 16.0).

linear relationship is totally different from the exponential relationship in conventional superconductors.

We also plot the optimal T_c versus the inverse local repulsion at varying values of $|V|$ (0.1, 0.2, 0.3, 0.5, 1.0, 2.0) in Fig. 3, together with the optimal doping. It can be observed that increasing the local repulsion can enhance T_c . This enhancement is more significant when $|V|$ is relatively small, while it becomes less pronounced for strong nearest-neighbor attraction.

C. Possible origin of high T_c : Role of density of states

It is important to emphasize that the parameter U does not manifest explicitly in the gap equation. Instead, its influence on the critical temperature T_c is mediated by its effects on the electronic band structure. To elucidate this mechanism, we present the density of states for various parameter sets (at optimal dopings), depicted in Fig. 4. Notably, the density of states reveals a pronounced VHS situated in close proximity to the Fermi energy. This proximity potentially underpins the heightened T_c observed in the extended Hubbard model.

To understand this relationship, we simplify the gap equation (16) in the limiting AFM case where $Um \gg 4t$. The gap

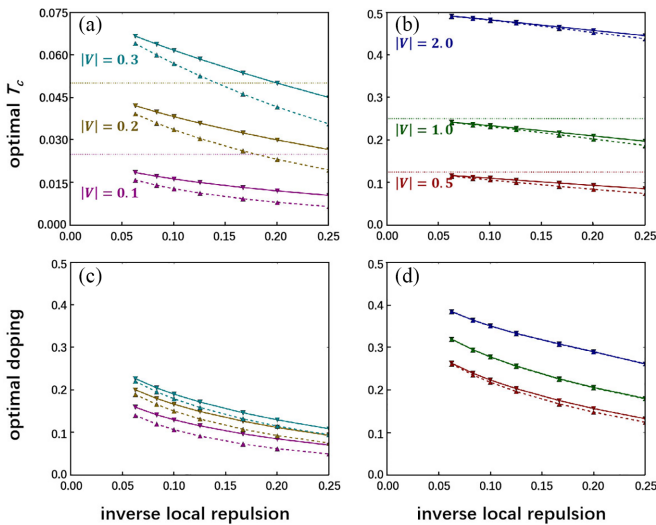


FIG. 3. Optimal critical temperature and hole doping versus the inverse local repulsion for d -wave instability (solid line) and p -wave instability (dashed line) at varying values of $|V|$ (0.1, 0.2, 0.3, 0.5, 1.0, 2.0).

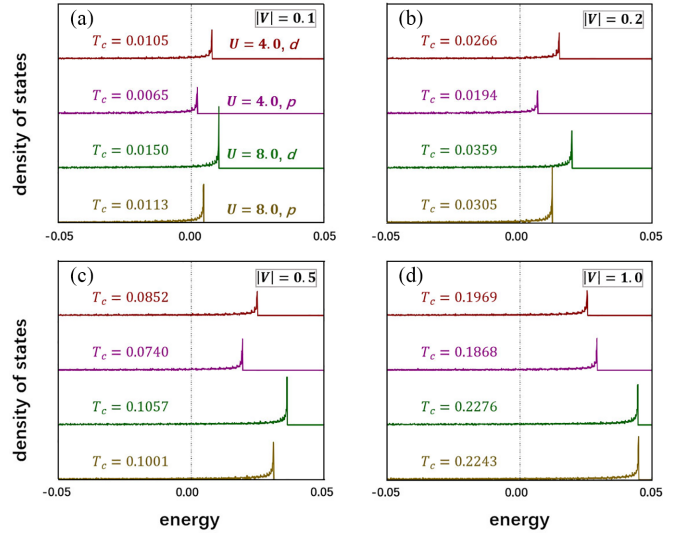


FIG. 4. The density of states for several sets of model parameters.

equation at T_c is then reduced to

$$\frac{1}{|V|} = \frac{1}{\mathcal{V}/2} \sum_p \phi_p^2 F_p^-. \quad (18)$$

Due to the presence of VHSs, we derive an estimation for T_c ,

$$T_c \sim \frac{N_0|V|}{4} \frac{x}{\operatorname{arctanh} x}, \quad (19)$$

with $x = 2\omega_0/N_0|V|$. Here N_0 represents the ratio of the number of states within the energy range $(-\omega_0, \omega_0)$ to that in the lower energy band, and ω_0 can be set as the energy difference between the VHS and the Fermi energy. Note that Eq. (19) is applicable only when $N_0|V| > 2\omega_0$. In the case $N_0|V| \gg 2\omega_0$, $T_c \sim N_0|V|/4$; that is, T_c is proportional to $|V|$.

IV. DISCUSSION

It is essential to acknowledge that mean-field methods have significant limitations when applied to two-dimensional Hubbard-like models. To address this, we reevaluate our numerical findings in light of existing experimental and theoretical results.

Dome-shaped feature. The critical temperature of hole-doped cuprate superconductors indeed exhibits a dome-shaped dependence on doping [3]. However, in the case of light doping, cuprates do not exhibit SC behavior, which contrasts with our numerical results. In comparison to Micas *et al.*'s work [32], where neglecting U resulted in the highest T_c occurring at half filling, we infer that the emergence of the dome-shaped feature is due to the influence of U . In our study, the effect of U is manifested in the density of states; however, at higher orders of perturbation theory, U would introduce corrections to the vertices. The absence of corrections to U might account for the deviations between our numerical results and existing experimental findings.

d-wave preference. Many hole-doped cuprate superconductors exhibit d -wave features [4], which are consistent with our numerical results. Based on our findings and Micas *et al.*'s work [32], the d -wave symmetry arises from the

competition among various nonlocal pairing channels, with their instability driven by the nearest-neighbor attractions. In the context of spin-fluctuation theory [14], the SC instability arising from strong local repulsion is also characterized by a d -wave symmetry in the order parameter.

Proportionality $T_c \propto |V|$. Although not observed in cuprates, evidence of such a proportional relationship exists at the FeSe/SrTiO₃ surface [37]. The BCS theory on a flat-band lattice is theoretically expected to result in this proportionality [25], and our work provides further support for this hypothesis. We believe that two key factors contributing to high T_c are the presence of a broad flat band near the Fermi surface and a sufficiently strong effective intersite attraction.

Existence of a flat band. The hole-doped cuprate superconductors exhibit partial flat bands near the Fermi surface [38], possibly originating from VHSs. Our numerical results also demonstrate the presence of flat bands and underscore their fundamental role in enhancing T_c . Moreover, many unconventional superconductors exhibit flat-band characteristics [39,40], implying that flat bands may be a common feature in unconventional superconductors.

Coexistence of AFM and SC orders. Since we assumed an AFM tendency in constructing the mean-field equations, the SC order emerges in the presence of AFM order within a broad range of doping levels. The coexistence of these two orders was also previously investigated in Ref. [34] at the mean-field level. This result differs from the phase diagram for hole-doped cuprates [3], where AFM order exists only at light doping levels (less than 0.05 usually). However, strong spin fluctuations are believed to exist within a broad range of doping levels.

Towards pairing density wave. The AFM order breaks the spin $SU(2)$ and spatial symmetries, resulting in SC order subject to spatial modulation, i.e., $\Delta'_{\delta,r} = \Delta'_{\delta,0} + \Delta'_{\delta,Q} e^{iQ \cdot r}$. The nonzero value of $\Delta'_{\delta,Q}$ corresponds to the pairing operator $\hat{c}_{\downarrow,k} \hat{c}_{\uparrow,Q-k}$, indicating a pairing density wave with momentum Q [41]. In our mean-field calculations, Δ'_Q is nonzero only when $m \neq 0$, implying that the pairing density wave emerges only in the presence of the AFM order. We may speculate that in a more precise computation of the extended Hubbard model, pairing density waves arise from strong spin-density-wave fluctuations.

Towards pseudogap. When both AFM (antiferromagnetic) and SC (superconducting) orders coexist, two distinct single-particle gaps emerge: the SC gap and the AFM gap. The pseudogap is commonly considered a precursor to an actual gap and can be generated by both SC and spin fluctuations [42,43]. In the extended Hubbard model, it is possible for two types of pseudogaps to coexist.

V. SUMMARY

In summary, we have explored the SC features on the extended Hubbard model at the mean-field level, assuming the system's inclination towards AFM order. Our numerical investigations have revealed several key features, including a predisposition towards d -wave pairing, the presence of a dome-shaped dependence of T_c on doping, an upper limit of

$0.25|V|$ for T_c with increasing U , and a nearly proportional relationship between T_c and $|V|$. By examining the system's density of states, we identified the existence of VHSs near the Fermi surface, which may serve as a prominent source of high-temperature superconductivity. These results suggest that the extended Hubbard model could be the appropriate framework for investigating cuprate superconductivity and are believed to offer insights for more precise calculations within this model in the future.

Based on our mean-field results, the presence of flat bands and strong electron-phonon interactions may be two crucial factors contributing to the high T_c . However, if so, there are several issues that warrant further investigation. These include completing a comprehensive mean-field analysis [44], considering higher-order perturbation theories [14], and incorporating dynamic effective attractions [30]. It is crucial to note that flat bands combined with strong interactions can introduce various correlated effects, and simple perturbation theory may not yield quantitatively satisfactory results. Further research is needed to address these challenges adequately.

APPENDIX: GAP EQUATION FOR PURE s -WAVE PAIRING

For pure s -wave pairing, the system of gap equations is given by

$$\begin{aligned} X_{0,\gamma} = & + \frac{|V|}{\mathcal{V}} \sum_{p'} \gamma_{p'}^2 (F_{p'}^- + F_{p'}^+) X_{0,\gamma} \\ & - \frac{|V|}{\mathcal{V}} \sum_{p'} \gamma_{p'}^2 (F_{p'}^- - F_{p'}^+) \sin \theta_{p'} X_{Q,\gamma} \\ & - \frac{U}{\mathcal{V}} \sum_{p'} \gamma_{p'} (F_{p'}^- - F_{p'}^+) \cos \theta_{p'} \Delta, \end{aligned} \quad (\text{A1a})$$

$$\begin{aligned} X_{Q,\gamma} = & - \frac{|V|}{\mathcal{V}} \sum_{p'} \gamma_{p'}^2 \sin \theta_{p'} (F_{p'}^- - F_{p'}^+) X_{0,\gamma} \\ & + \frac{|V|}{\mathcal{V}} \sum_{p'} \gamma_{p'}^2 [\sin^2 \theta_{p'} (F_{p'}^- + F_{p'}^+) + 2 \cos^2 \theta_{p'} F_{p'}'] X_{Q,\gamma} \\ & + \frac{U}{\mathcal{V}} \sum_{p'} \gamma_{p'} (F_{p'}^- + F_{p'}^+ - 2F_{p'}') \sin \theta_{p'} \cos \theta_{p'} \Delta, \end{aligned} \quad (\text{A1b})$$

$$\begin{aligned} \Delta = & + \frac{|V|}{\mathcal{V}} \sum_{p'} (F_{p'}^- - F_{p'}^+) \cos \theta_{p'} X_{0,\gamma} \gamma_{p'} \\ & - \frac{|V|}{\mathcal{V}} \sum_{p'} (F_{p'}^- + F_{p'}^+ - 2F_{p'}') \sin \theta_{p'} \cos \theta_{p'} X_{Q,\gamma} \gamma_{p'} \\ & - \frac{U}{\mathcal{V}} \sum_{p'} (\cos^2 \theta_{p'} (F_{p'}^- + F_{p'}^+) + 2 \sin^2 \theta_{p'} F_{p'}') \Delta. \end{aligned} \quad (\text{A1c})$$

For most parameters under consideration, T_c for the s -wave pairing instability is smaller than those for d and p pairing instabilities. This is because the s -wave pairing instability will be suppressed by the local repulsion.

- [1] R. Micnas, J. Ranninger, and S. Robaszkiewicz, Superconductivity in narrow-band systems with local nonretarded attractive interactions, *Rev. Mod. Phys.* **62**, 113 (1990).
- [2] D. J. Scalapino, A common thread: The pairing interaction for unconventional superconductors, *Rev. Mod. Phys.* **84**, 1383 (2012).
- [3] J. A. Sobota, Y. He, and Z.-X. Shen, Angle-resolved photoemission studies of quantum materials, *Rev. Mod. Phys.* **93**, 025006 (2021).
- [4] C. C. Tsuei and J. R. Kirtley, Pairing symmetry in cuprate superconductors, *Rev. Mod. Phys.* **72**, 969 (2000).
- [5] J. G. Bednorz and K. A. Müller, Possible high T_c superconductivity in the Ba-La-Cu-O system, *Z. Phys. B* **64**, 189 (1986).
- [6] J. Bardeen, L. N. Cooper, and J. R. Schrieffer, Theory of superconductivity, *Phys. Rev.* **108**, 1175 (1957).
- [7] W. L. McMillan, Transition temperature of strong-coupled superconductors, *Phys. Rev.* **167**, 331 (1968).
- [8] H. Keller, Unconventional isotope effects in cuprate superconductors, *Struct. Bonding (Berlin, Ger.)* **114**, 143 (2005).
- [9] G.-M. Zhao, H. Keller, and K. Conder, Unconventional isotope effects in the high-temperature cuprate superconductors, *J. Phys.: Condens. Matter* **13**, R569 (2001).
- [10] T. Timusk and B. Statt, The pseudogap in high-temperature superconductors: An experimental survey, *Rep. Prog. Phys.* **62**, 61 (1999).
- [11] J. M. Tranquada, Cuprate superconductors as viewed through a striped lens, *Adv. Phys.* **69**, 437 (2020).
- [12] P. W. Phillips, N. E. Hussey, and P. Abbamonte, Stranger than metals, *Science* **377**, eabh4273 (2022).
- [13] P. W. Anderson, The resonating valence bond state in La_2CuO_4 and superconductivity, *Science* **235**, 1196 (1987).
- [14] N. E. Bickers, D. J. Scalapino, and S. R. White, Conserving approximations for strongly correlated electron systems: Bethe-Salpeter equation and dynamics for the two-dimensional Hubbard model, *Phys. Rev. Lett.* **62**, 961 (1989).
- [15] H. Q. Lin, J. E. Hirsch, and D. J. Scalapino, Pairing in the two-dimensional Hubbard model: An exact diagonalization study, *Phys. Rev. B* **37**, 7359 (1988).
- [16] M. Qin, C.-M. Chung, H. Shi, E. Vitali, C. Hubig, U. Schollwöck, S. R. White, and S. Zhang, Absence of superconductivity in the pure two-dimensional Hubbard model, *Phys. Rev. X* **10**, 031016 (2020).
- [17] H. Xu, C.-M. Chung, M. Qin, U. Schollwöck, S. R. White, and S. Zhang, Coexistence of superconductivity with partially filled stripes in the Hubbard model, [arXiv:2303.08376](https://arxiv.org/abs/2303.08376).
- [18] N. Singh, Leading theories of the cuprate superconductivity: A critique, *Physica C (Amsterdam, Neth.)* **580**, 1353782 (2021).
- [19] B. Keimer, S. A. Kivelson, M. R. Norman, S. Uchida, and J. Zaanen, From quantum matter to high-temperature superconductivity in copper oxides, *Nature (London)* **518**, 179 (2015).
- [20] L. P. Gor'kov and V. Z. Kresin, *Colloquium*: High pressure and road to room temperature superconductivity, *Rev. Mod. Phys.* **90**, 011001 (2018).
- [21] A. A. Abrikosov, J. C. Campuzano, and K. Gofron, Experimentally observed extended saddle point singularity in the energy spectrum of $\text{YBa}_2\text{Cu}_3\text{O}_{6.9}$ and $\text{YBa}_2\text{Cu}_4\text{O}_8$ and some of the consequences, *Phys. C (Amsterdam, Neth.)* **214**, 73 (1993).
- [22] E. Dagotto, A. Nazarenko, and A. Moreo, Antiferromagnetic and Van Hove scenarios for the cuprates: Taking the best of both worlds, *Phys. Rev. Lett.* **74**, 310 (1995).
- [23] R. S. Markiewicz, B. Singh, C. Lane, and A. Bansil, Investigating the cuprates as a platform for high-order Van Hove singularities and flat-band physics, *Commun. Phys.* **6**, 292 (2023).
- [24] D. M. Newns, C. C. Tsuei, and P. C. Pattnaik, Van Hove scenario for d -wave superconductivity in cuprates, *Phys. Rev. B* **52**, 13611 (1995).
- [25] S. Miyahara, S. Kusuta, and N. Furukawa, BCS theory on a flat band lattice, *Phys. C (Amsterdam, Neth.)* **460–462**, 1145 (2007).
- [26] T. T. Heikkilä and G. E. Volovik, Flat bands as a route to high-temperature superconductivity in graphite, in *Basic Physics of Functionalized Graphite* (Springer International Publishing, Cham, 2016), pp. 123–143.
- [27] G. E. Volovik, Flat band in topological matter: Possible route to room-temperature superconductivity, *J. Supercond. Novel Magn.* **26**, 2887 (2013).
- [28] Z. Chen, Y. Wang, S. N. Rebec, T. Jia, M. Hashimoto, D. Lu, B. Moritz, R. G. Moore, T. P. Devereaux, and Z.-X. Shen, Anomalous strong near-neighbor attraction in doped 1D cuprate chains, *Science* **373**, 1235 (2021).
- [29] T. Tang, B. Moritz, C. Peng, Z.-X. Shen, and T. P. Devereaux, Traces of electron-phonon coupling in one-dimensional cuprates, *Nat. Commun.* **14**, 3129 (2023).
- [30] Y. Wang, Z. Chen, T. Shi, B. Moritz, Z.-X. Shen, and T. P. Devereaux, Phonon-mediated long-range attractive interaction in one-dimensional cuprates, *Phys. Rev. Lett.* **127**, 197003 (2021).
- [31] M. Kheirkhah, Z. Yan, Y. Nagai, and F. Marsiglio, First- and second-order topological superconductivity and temperature-driven topological phase transitions in the extended Hubbard model with spin-orbit coupling, *Phys. Rev. Lett.* **125**, 017001 (2020).
- [32] R. Micnas, J. Ranninger, S. Robaszkiewicz, and S. Tabor, Superconductivity in a narrow-band system with intersite electron pairing in two dimensions: A mean-field study, *Phys. Rev. B* **37**, 9410 (1988).
- [33] W. P. Su, Phase separation and d -wave superconductivity in a two-dimensional extended Hubbard model with nearest-neighbor attractive interaction, *Phys. Rev. B* **69**, 012506 (2004).
- [34] B. Tobijaszevska and R. Micnas, Competition of d -wave superconductivity and antiferromagnetism in the extended Hubbard model, superfluid properties, *Phys. Stat. Sol. (b)* **242**, 468 (2005).
- [35] M. Jiang, Enhancing d -wave superconductivity with nearest-neighbor attraction in the extended Hubbard model, *Phys. Rev. B* **105**, 024510 (2022).
- [36] C. Peng, Y. Wang, J. Wen, Y. S. Lee, T. P. Devereaux, and H.-C. Jiang, Enhanced superconductivity by near-neighbor attraction in the doped extended Hubbard model, *Phys. Rev. B* **107**, L201102 (2023).
- [37] Q. Song, T. L. Yu, X. Lou, B. P. Xie, H. C. Xu, C. H. P. Wen, Q. Yao, S. Y. Zhang, X. T. Zhu, J. D. Guo, R. Peng, and D. L. Feng,

- Evidence of cooperative effect on the enhanced superconducting transition temperature at the FeSe/SrTiO₃ interface, *Nat. Commun.* **10**, 758 (2019).
- [38] Z.-X. Shen and D. S. Dessau, Electronic structure and photoemission studies of late transition-metal oxides—Mott insulators and high-temperature superconductors, *Phys. Rep.* **253**, 1 (1995).
- [39] Y. Cao, V. Fatemi, S. Fang, K. Watanabe, T. Taniguchi, E. Kaxiras, and P. Jarillo-Herrero, Unconventional superconductivity in magic-angle graphene superlattices, *Nature (London)* **556**, 43 (2018).
- [40] V. R. Shaginyan, A. Z. Msezane, and G. S. Japaridze, Peculiar physics of heavy-fermion metals: Theory versus experiment, *Atoms* **10**, 67 (2022).
- [41] Note that in Ref. [34], $\Delta'_{\delta,\mathbf{Q}}$ was interpreted as the order parameter for the π triplet. However, since the $SU(2)$ symmetry is broken, $\Delta'_{\delta,\mathbf{Q}}$ should not refer to a triplet.
- [42] Q. Chen, J. Stajic, S. Tan, and K. Levin, BCS–BEC crossover: From high temperature superconductors to ultracold superfluids, *Phys. Rep.* **412**, 1 (2005).
- [43] T. Schäfer *et al.*, Tracking the footprints of spin fluctuations: A multimethod, multimessenger study of the two-dimensional Hubbard model, *Phys. Rev. X* **11**, 011058 (2021).
- [44] M. Kato, K. Machida, H. Nakanishi, and M. Fujita, Soliton lattice modulation of incommensurate spin density wave in two dimensional Hubbard model -A mean field study-, *J. Phys. Soc. Jpn.* **59**, 1047 (1990).